Chapter 7 QCD and Two-Photon Physics

1 Introduction

A relatively clean environment and well-understood initial-state parton content render e^+e^- colliding beam experiments ideal for both the qualitative confirmation and quantitative testing of Quantum Chromodynamics (QCD). Through the years, a number of seminal discoveries and measurements performed at e^+e^- colliding beam facilities have served to establish the SU(3) color gauge theory QCD as the accepted dynamical model of the strong nuclear interaction. Highlights unique to the e^+e^- QCD program include the discovery of the gluon at PETRA in 1979, the confirmation of the SU(3) gauge structure of quark-gluon and gluon-gluon vertices at LEP in the early 1990s, and the precise measurement of the strong coupling constant α_s from hadronic observables and from the Z and τ decay widths.

The study of QCD, and the dynamics of the strong force in general, is expected to provide a significant contribution to the physics program at a high-energy e^+e^- colliding beam facility. The highlights of this program include

- the precise determination of the strong coupling constant α_s;
- the search for anomalous strong couplings of the top quark;
- the study of photon structure; and
- the study of strong-interaction dynamics at high $\sqrt{s}$ and fixed t.

Together, these measurements probe some of the most important topics in the study of strong force dynamics, in ways that are often superior to measurements at hadron colliders.

2 QCD from annihilation processes

2.1 The precise determination of α_s

As the single free parameter of the SU(3) gauge theory of the strong interaction, the strong coupling constant α_s should be measured to the highest available precision. Renormalization group extrapolations of the U(1), SU(2) and SU(3) coupling strengths constrain physics scenarios at the GUT scale. The current constraints are limited by the few-percent relative precision [1] of the value of $\alpha_s(m_Z^2)$. The value of α_s should also be determined with comparable accuracy over as large a range of scales as possible in order to measure the renormalization-group running of α_s and to reveal potential anomalous running in the strength of the strong interaction. In this article, as a matter of convention, measurements of α_s performed at other scales

will be evolved to the scale $Q^2 = M_Z^2$ according to Standard Model renormalization group equations and quoted in terms of their implied value of $\alpha_s(m_Z^2)$.

2.1.1 Event observables in e^+e^- annihilation

The determination of $\alpha_s(m_Z^2)$ from the process $e^+e^- \to Z/\gamma \to q\overline{q}(g)$, using 'shape' observables that are sensitive to the underlying parton content, has been pursued for two decades and is generally well understood [2]. In this method one usually forms a differential distribution, makes corrections for detector and hadronization effects, and fits a perturbative QCD prediction to the data, allowing $\alpha_s(m_Z^2)$ to vary. Examples of such observables are thrust, jet masses and jet rates.

The latest generation of such $\alpha_s(m_Z^2)$ measurements, from SLC and LEP, has shown that statistical errors below the 1% level can be obtained with samples of a few tens of thousands of hadronic events. With the current linear collider design luminosity of 2.2×10^{34} cm^{-2}s^{-1}, at $\sqrt{s} = 500$ GeV, hundreds of thousands of $e^+e^- \to q\overline{q}$ events would be produced each year, and a statistical error on $\alpha_s(m_Z^2)$ below 0.5% would be achieved.

At energies far above the Z pole, the electron-positron collision cross section is dominated by t-channel processes such as ZZ and W^+W^- production. In addition, because of the substantial mass of the t quark, the inclusive characteristics of $e^+e^- \to t\overline{t}$ events tend to mimic those of lighter quark events with hard gluon radiation. A prescription for the elimination of these backgrounds was developed for the 1996 Snowmass workshop [3,4]. This prescription makes use of electron beam polarization and precise tracking to reduce the effects of these backgrounds on the measured three-jet rate to less than 5%, with the corresponding systematic uncertainty on the extraction of $\alpha_s(m_Z^2)$ expected to be substantially less than 1%. The sizable initial-state and beamstrahlung radiation associated with linear collider energies will act to smear the CM energy of the e^+e^- annihilation process, as well as to boost the particle flow into the forward regions of the detector. A PYTHIA study [5], including the full effects of ISR, has shown that these considerations can be accurately taken into account in the measurement of $\alpha_s(m_Z^2)$.

Hadronization effects, which lead to corrections of order 10% at the Z^0 pole, are expected to fall at least as fast as $1/\sqrt{s}$, leading to corrections of order 1% at $\sqrt{s} \geq$ 500 GeV [6]. The corresponding systematic error on the extraction of $\alpha_s(m_Z^2)$ is thus expected to be substantially below 1%. Detector systematics, due primarily to limited acceptance and resolution smearing, and which are observable-dependent, are found to contribute at the level of $\delta\alpha_s(m_Z^2)$= $\pm$1–4% at LEP-II [7]. The greater hermeticity and $\cos\theta$ coverage anticipated for linear collider detectors are again expected to reduce this substantially.

Currently, perturbative calculations of event shapes are complete only up to $O(\alpha_s^2)$, although resummed calculations are available for some observables [8]. One must

therefore estimate the possible bias inherent in measuring $\alpha_s(m_Z^2)$ using the truncated QCD series. Though not universally accepted, it is customary to estimate this from the dependence of the fitted $\alpha_s(m_Z^2)$ value on the QCD renormalization scale, yielding a large and dominant uncertainty of about $\Delta\alpha_s(m_Z^2) \simeq \pm 6\%$ [2]. Therefore, although a $\pm 1\%$-level $\alpha_s(m_Z^2)$ measurement is possible experimentally, it will not be realized until $O(\alpha_s^3)$ contributions are completed. There is a reasonable expectation that this will be achieved within the next three years [9,10].

2.1.2 The $t\bar{t}(g)$ system

The dependence of the $e^+e^- \to t\bar{t}$ cross section on m_t and $\alpha_s(m_Z^2)$ is presented in Chapter 6, Section 2. As discussed there, next-to-next-to-leading-order calculations of the $t\bar{t}$ cross section in the resonance region show convergence to the few-percent level for an appropriate definition of m_t, if logarithms of the top quark velocity are resummed. This is good news for the extraction of m_t; however, we will probably not obtain a competitive value of $\alpha_s(m_Z^2)$ from this system.

2.1.3 A high-luminosity run at the Z^0 resonance

A sample of 10^9 Z^0 decays offers two additional options for the determination of $\alpha_s(m_Z^2)$ via measurements of the inclusive ratios $\Gamma_Z^{\rm had}/\Gamma_Z^{\rm lept}$ and $\Gamma_\tau^{\rm had}/\Gamma_\tau^{\rm lept}$. In both cases, α_s enters in through the QCD radiative correction; thus, both observables require a very large event sample for a precise measurement. For example, the current LEP data sample of 16M Z^0 decays yields an error of $\pm 2.5\%$ on $\alpha_s(m_Z^2)$ from $\Gamma_Z^{\rm had}/\Gamma_Z^{\rm lept}$, with an experimental systematic of $\pm 1\%$. With a Giga-Z sample, the statistical error would be pushed to below $\Delta\alpha_s(m_Z^2) = 0.4\%$. Even with no improvement in experimental systematics, this would be a precise and reliable measurement. In the case of $\Gamma_\tau^{\rm had}/\Gamma_\tau^{\rm lept}$ the experimental precision from LEP and CLEO is already at the 1% level on $\alpha_s(m_Z^2)$. However, there has been considerable debate about the size of the theoretical uncertainties, with estimates as large as 5% [11]. If this situation is clarified, and the theoretical uncertainty is small, $\Gamma_\tau^{\rm had}/\Gamma_\tau^{\rm lept}$ may offer a further 1%-level $\alpha_s(m_Z^2)$ measurement.

2.2 Q^2 evolution of α_s

In the preceding sections we discussed the expected precision on the measurement of the benchmark parameter $\alpha_s(m_Z^2)$. Translation of the measurements of $\alpha_s(Q^2)$ ($Q^2 \neq M_Z^2$) to $\alpha_s(m_Z^2)$ requires the assumption that the 'running' of the coupling is determined by the QCD β function. However, since the logarithmic decrease of α_s with Q^2 is a telling prediction of QCD, reflecting the underlying non-Abelian dynamics, it is essential to test this Q^2 dependence explicitly. In particular, such a

test would be sensitive to new colored degrees of freedom with mass below the limit for pair production at the highest explored scale. For this measurement of the Q^2-dependence of α_s, rather than its overall magnitude, many common systematic effects would be expected to cancel. Hence it would be desirable to measure α_s in the same detector, with the same technique, and by applying the same treatment to the data at a series of different Q^2 scales, so as to maximize the lever-arm for constraining the running.

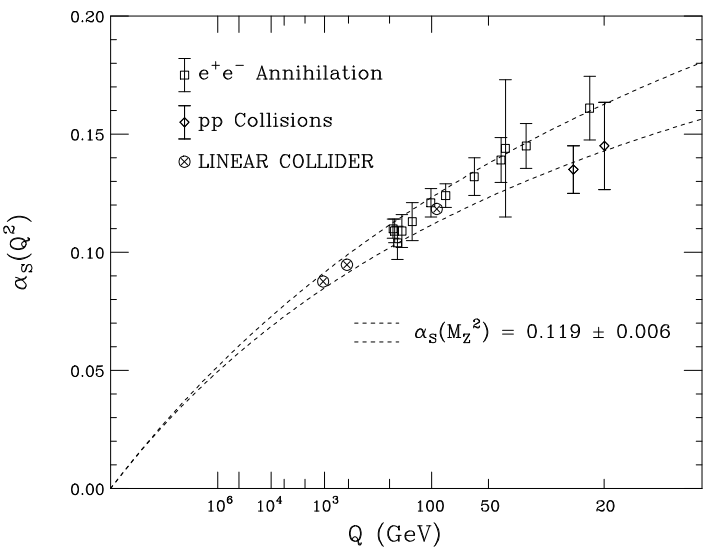

Figure 7.1: Linear collider measurements of $\alpha_s(m_Z^2)$, in comparison to existing measurements from e^+e^- and $p\overline{p}$ collisions, as a function of interaction scale.

Proposed linear collider measurements of $\alpha_s(Q^2)$ at $\sqrt{s} = 91$, 500 and 1000 GeV are shown in Fig. 7.1, together with existing measurements which span the range $20 \leq \sqrt{s} \leq 200$ GeV. The linear collider point at $\sqrt{s} = 91$ GeV can be obtained either from jet rates or from the $\Gamma_Z^{\rm had}/\Gamma_Z^{\rm lept}$ technique, while those at 500 and 1000 GeV are based on jet rates. A theoretical uncertainty of $\pm 1\%$ is assumed for all LC points.

The linear collider data would add significantly to the lever-arm in Q^2, and would allow a substantially improved extrapolation to the GUT scale. Consider, for example, making a simultaneous fit for $\alpha_s(m_Z^2)$ and for β_0, the leading term in the expansion of the QCD β-function which establishes the rate at which the strong coupling constant runs. (This term is expected to be about 0.61 in the SM.) The linear collider data alone would give a precision on these quantities of ± 0.0018 and ± 0.034, respectively. Including accurate measurements at low Q^2 (particularly from e and μ deep inelastic scattering), the existing constraints are ± 0.0030 and ± 0.042, respectively. Combining existing data with that available from the LC would yield constraints of ± 0.0009 and

± 0.016, providing a substantial improvement on the measurement of the running of $\alpha_s(m_Z^2)$, as well as the extrapolation to the GUT scale (see Fig. 7.2). Note that, unlike the determination of β_0, the accuracy of the GUT-scale extrapolation is not dependent upon future running at the Z^0.

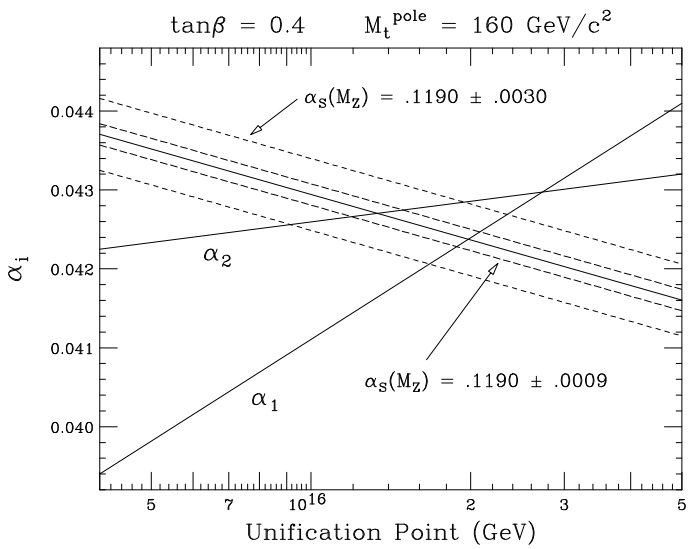

Figure 7.2: Improvement in the GUT scale constraint, assuming a $\pm 1\%$ measurement of $\alpha_s(m_Z^2)$ at the linear collider. Renormalization group trajectories assume the MSSM with $\tan\beta = 0.4$ and $m_t^{\rm pole} = 160$ GeV [12].

2.3 Top quark strong moments

The very large mass of the recently discovered top quark suggests the possibility that top plays a central role in physics beyond the Standard Model. If this is the case, it is likely that this new physics will manifest itself via anomalous top-quark moments, which represent the low-energy manifestation of effective higher-dimensional couplings. The measurement of the electroweak anomalous moments of the top quark is discussed in Chapter 6, Section 3.3.

In the case of the strong interactions of top, the lowest-dimensional gauge-invariant and CP-conserving extension to SM top quark couplings is the anomalous chromomagnetic moment, which we can parameterize via a dimensionless quantity κ. The corresponding chromoelectric moment, parameterized by $\tilde{\kappa}$, violates CP and arises from an operator of the same dimension. The resulting generalized three-point $t\bar{t}g$ vertex takes the form

$$L = g_s \bar{t} T_a \left(\gamma_\mu + \frac{i}{2m_t} \sigma_{\mu\nu} (\kappa - i\tilde{\kappa}\gamma_5) q^\nu \right) t G_a^\mu, \tag{7.1}$$

where g_s is the SU(3) gauge coupling parameter, m_t is the top quark mass, T_a are the SU(3) color generators, G_a^μ are the vector gluon fields, and q is the outgoing gluon four-momentum.

This interaction leads to a substantially different spectrum of gluon radiation for $e^+e^- \to t\bar{t}$ events above threshold than for the pure vector interaction case corresponding to $\kappa = \tilde{\kappa} = 0$. Fits to this spectrum thus provide limits on the values of κ and $\tilde{\kappa}$. Figure 7.3, from Ref. [13], shows the limits in the κ-$\tilde{\kappa}$ plane that can be achieved with an integrated luminosity of 100 and 200 fb^{-1} at $\sqrt{s} = 1$ TeV. Similar studies for the Tevatron and LHC [14] indicate that the corresponding sensitivities at hadron colliders will be substantially weaker, in particular for the case of κ, for which sensitivities of $|\kappa| < 0.1$ will be difficult to achieve. In [15], the authors offer a technicolor model for which the unique capability of the LC to measure strong moments of top precisely would be a critical asset.

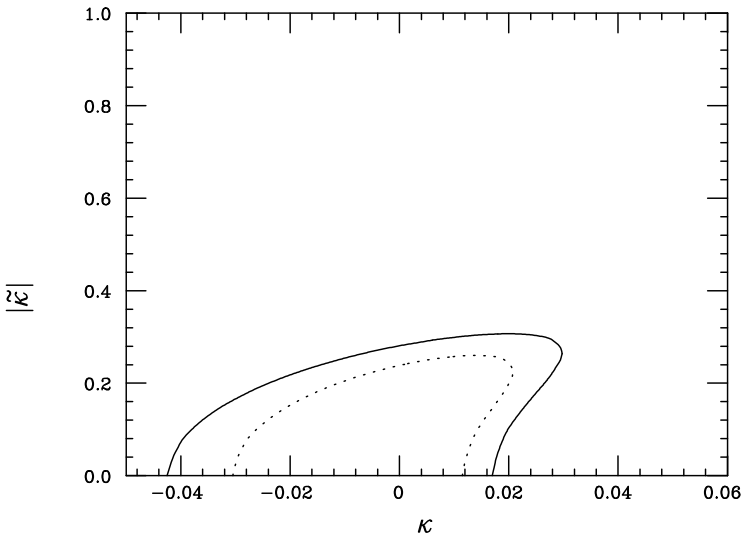

Figure 7.3: Constraints on anomalous strong moments of the top quark, derived from a LC sample of 100 fb^{-1} (solid) and 200 fb^{-1} (dotted) for $\sqrt{s} = 1$ TeV.

3 Two-photon physics

At a future e^+e^- linear collider, we will be able to study the two-photon processes $e^+e^- \to e^+e^- + \gamma^{(*)}\gamma^{(*)} \to e^+e^- +$ hadrons for all combinations of real (γ) and virtual (γ^*) photons. Reactions of real photons can also be studied by using a dedicated backscattered-laser photon beam, as described in Chapter 13. These reactions test QCD in photon structure measurements and in the dynamics of parton distribution

function evolution. Direct measurement of the photon structure function $F_2^\gamma(x, Q^2)$ in $\gamma\gamma^*$ collisions pushes into currently unattainable regimes of lower x and higher Q^2, testing scaling behavior and Q^2 evolution. Extending the measurement of the total $\gamma\gamma$ cross section to higher $\sqrt{s}$ tests whether QCD-based models of parton emission describe photon interactions. By colliding two virtual photons, QCD dynamics can be studied in a relatively background-free environment. No other planned or anticipated future collider will be able to compete with an e^+e^- linear collider in these areas.

We now present a comprehensive plan for the study of photon structure through $e\gamma$ deep inelastic scattering (DIS) and $\gamma\gamma$ scattering, and through the study of QCD dynamics through $\gamma^*\gamma^*$ scattering. We discuss the relative merits of employing photons produced by bremsstrahlung and laser backscattering and the utility of having well-defined photon polarization.

3.1 Experimental requirements

Experimental issues related to two-photon physics are mainly concerned with instrumentation of the forward parts of the interaction region (IR), particularly inside the conical shielding masks. The cases in which the initial photons are produced by bremsstrahlung from e^+e^- and from laser backscattering have some differences, but also many similarities.

3.2 Bremsstrahlung photon beam

In an IR designed for e^+e^- collisions, the study of two-photon processes requires small-angle-tagging electromagnetic calorimeters in the forward regions. Some physics topics also require hadronic calorimetry from beampipe to beampipe.

Virtual photons are produced when, in the bremsstrahlung process, an e^+ or e^- transfers a significant amount of 4-momentum to the radiated photon. The virtuality, Q^2, of the "tagged" photon is determined by measuring the energy and angle of the scattered lepton in an electromagnetic calorimeter via the relation

$$Q^2 = 2E_eE'_e(1 - \cos\theta) \ , \tag{7.2}$$

where E_e is the incoming lepton beam energy, and E'_e and θ are the scattered lepton energy and angle, respectively. Since some physics analyses require that the measurement of Q^2 be as small as possible, the electromagnetic tagging calorimeters must be positioned as closely as possible to the outgoing beampipes on both sides of the interaction region and inside the shielding cone in order make the minimum measurable scattered lepton angle as small as possible, leading to the requirement of a compact design. Also, since $Q^2 \simeq E_eE'_e\theta^2$ at small angles, radial position resolution is an important consideration in Q^2 reconstruction, requiring fine-grained readout in the radial direction [16]. Fine-grained sampling calorimeters with these properties have been successfully used in photon-tagging experiments at LEP [17].

Almost-real photons ($Q^2 \simeq 0$) from the bremsstrahlung process are defined by anti-tags in the forward electromagnetic tagging calorimeters. For example, a single tag on one side of the IR, combined with an anti-tag on the other side with hadronic activity in the main detector, signals a $\gamma^*\gamma$ interaction ($e\gamma$ DIS). Double anti-tags signal $\gamma\gamma$ interactions in which both interacting photons are almost real. It is important to note that the energy spectrum of bremsstrahlung-produced photons is dominated by low-energy photons. Furthermore, since the untagged photon energy is not known, it is important to have hadronic energy and angle measurement in the forward IR, to as small an angle as possible, in order to determine the kinematics of the interaction.

3.2.1 Backscattered laser beam

It would be desirable to create a beam of high-energy real photons by Compton backscattering of a high-power, high-repetition-rate laser from the electron beams. The technology for achieving this backscattered-laser photon beam is described in Chapter 13. To prepare the Compton-backscattered beam, 1 eV laser photons backscatter from the incoming 250 GeV e^- beam, producing a beam of photons carrying about 75% of the electron beam energy with an energy spread of 5–10%. Since the resulting photon beam energy spread is small, the kinematics of the high-energy photon interactions can be determined from the known photon energy. Also, since these are high-energy photons at nearly the incoming lepton beam energy, the mass of the two-photon system $W_{\gamma*\gamma}$ is much larger than that obtained from bremsstrahlung-produced photons, leading to the possibility of reaching very low x in $e\gamma$ DIS.

In addition, the polarization state of the interacting photons and/or leptons can have a big effect on the physics impact of a measurement. For example, by combining the circular polarizations of the incoming leptons and the laser photons in an optimal way, the energy spread of the resulting backscattered photon beam can be reduced by almost a factor of 2.

3.3 Photon structure

A real photon can interact both as a point-like particle, or as a collection of quarks and gluons, *i.e.*, like a hadron. The structure of the photon is determined not by the traditional valence quark distributions as in a proton, but by fluctuations of the point-like photon into a collection of partons. As such, the scaling behavior of the photon structure function, $dF_2^\gamma/d\ln Q^2$, is always positive. Single-tag and double-anti-tag events can be used to measure F_2^γ directly and to constrain the relative quark/gluon fractions in the photon, testing predictions for this content and its behavior.

3.3.1 $\gamma^*\gamma$ scattering—$e\gamma$ DIS

Direct measurement of the photon structure function $F_2^\gamma(x, Q^2)$ in $e\gamma$ DIS is accomplished by tagging a single virtual photon probe, anti-tagging an almost-real or real target photon, and requiring hadronic activity anywhere in the detector.

If the anti-tagged target photon is produced by bremsstrahlung from an incoming lepton, it has very small virtuality, $\langle Q^2 \rangle \simeq 10^{-4}$ GeV^2, and low energy, neither of which is known. In order to determine the longitudinal momentum fraction, x, the mass $W_{\gamma^*\gamma}$ of the $\gamma^*\gamma$ system must be measured, which requires hadronic calorimetry to measure the energy and angle of all hadrons. The best measurements of F_2^γ using bremsstrahlung photons as the target are done at relatively low $W_{\gamma^*\gamma}$ where it is well-measured away from the forward IR, which in kinematic space is at the high end of the x, Q^2 range. Physics topics that can best be addressed in this region are the scaling behavior of F_2^γ as $x \to 1$ and its evolution with Q^2.

As $W_{\gamma^*\gamma}$ increases (towards low x), increasingly more of the hadronic mass escapes undetected in the beam direction and the mass of the observed hadrons, usually referred to as $W_{\rm vis}$, begins to differ substantially from the true hadronic mass. Figure 7.4 illustrates this effect by comparing $W_{\rm vis}$ with the true mass, $W_{\gamma^*\gamma}$.

Monte Carlo simulations of the fragmentation of the $\gamma^*\gamma$ system are used to correct $W_{\rm vis}$ for this loss until the uncertainty in the correction begins to dominate the measurement. Eventually, this limits the low-x range of the F_2^γ measurement.

However, if the target photon is produced by laser backscattering, two advantages are realized: 1) the high $W_{\gamma^*\gamma}$ (low-x) region is enhanced since the real photon energy is high; and 2) the energy spread of the real photons is small enough that the error on x caused by assuming a monochromatic photon does not dominate the systematics.

Figure 7.5 shows F_2^γ versus Q^2 for various x bins from possible measurements at a future e^+e^- linear collider [20]. The various points are differentiated according to the measurement method. The open squares represent the very low-x region accessible only with photons produced by laser backscattering; open circles represent measurements with target photons from bremsstrahlung and with hadronic calorimetry built into a shielding mask down to 30 mrad; solid dots represent measurements with bremsstrahlung photons and with hadronic calorimetry only outside the mask. Note that there is enough overlap between the methods to provide cross-checks on the various measurements and experimental conditions.

With known polarization of both the target photon and the tagged virtual photon, polarized photon structure functions can be measured for the first time. The 'BFKL' terms involving $\ln(1/x)$ in the unpolarized structure functions enter in polarized scattering as $\ln^2(1/x)$. These effects are then enhanced at low x over the unpolarized case. Thus, in polarized $e\gamma$ DIS, forward particle and jet measurements, such as have been performed at HERA [21], can be done at a future e^+e^- linear collider with increased sensitivity to any BFKL effects.

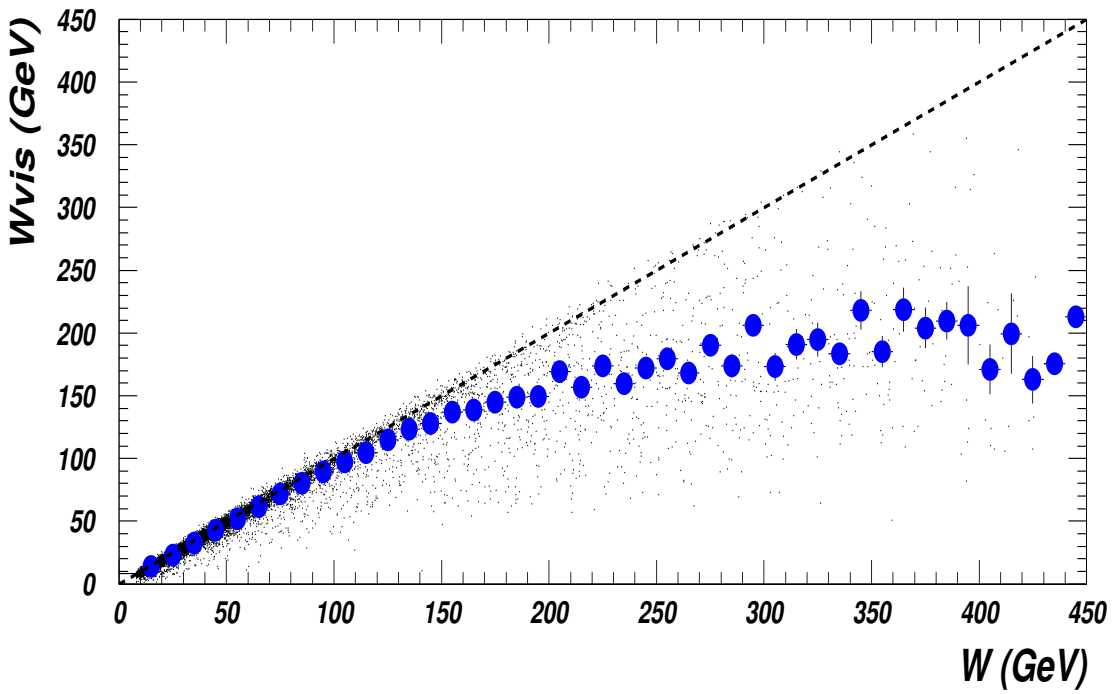

Figure 7.4: Comparison of W_{vis} with $W_{\gamma^*\gamma}$ from PYTHIA [19] for a typical LC detector, including the average value (profile plot).

In addition to the F_2^γ structure function, $e\gamma$ DIS can be used to test QCD in other ways. For example, dijet production in DIS can be used to extract the strong coupling parameter, α_s, as is done at HERA [22]. At a future e^+e^- linear collider, α_s from e^+e^- event shapes and from dijets in DIS can be compared using the same detector.

3.4 $\gamma\gamma$ scattering—total cross section

Various models have been developed to describe the rise with energy of the total $\gamma\gamma$ cross section. These give either a fast rise driven by QCD effects such as minijets, or a slower rise based on reggeon exchange. To get to the highest $\sqrt{s}$ and $W_{\gamma\gamma}$, real photons from the laser backscattering process are required. Studies show that a precision of $\sim 20\%$ on the total cross section will enable adequate discrimination of model types for energies up to 1 TeV [23]. Figure 7.6 shows possible σ_{tot} measurements at a 500 GeV linear collider (large stars) compared to existing measurements at lower $\sqrt{s}$ and to various models.

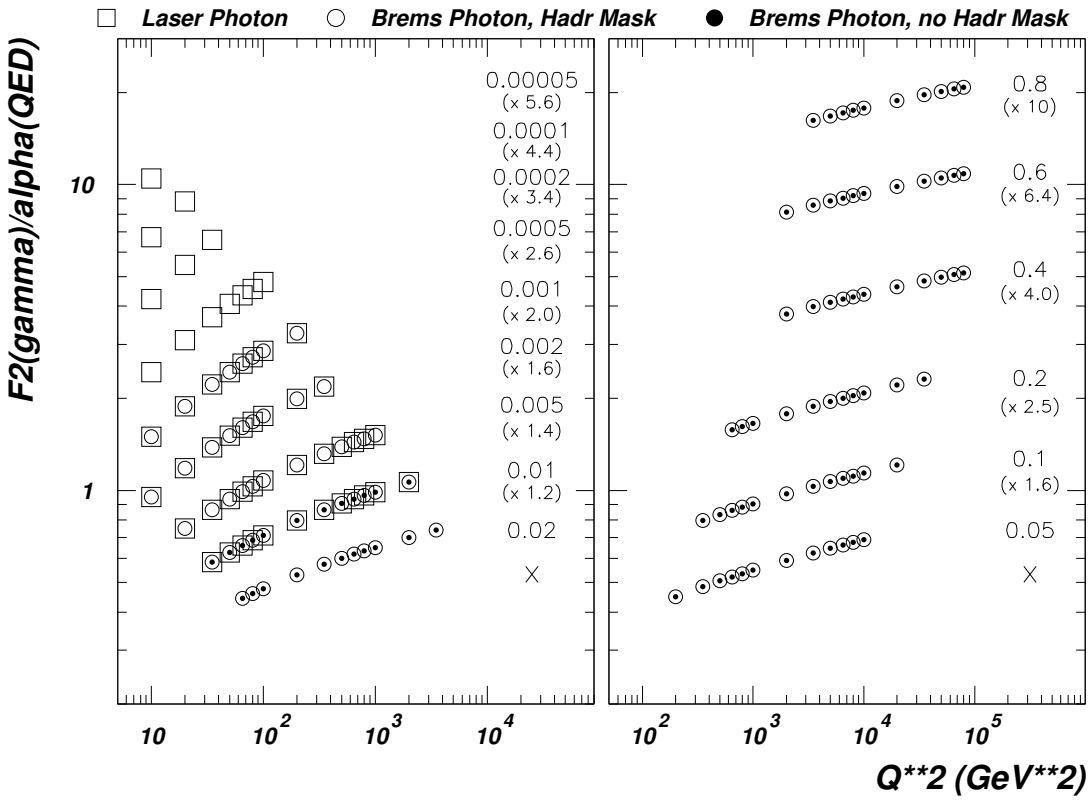

Figure 7.5: F_2^γ/α versus Q^2 in x bins. Open squares: real photon target from laser backscattering; open circles: almost-real photon target from bremsstrahlung with small-angle hadronic calorimetry; solid dots: almost-real photon target from bremsstrahlung with hadronic calorimetry outside mask.

Using dijets from $\gamma\gamma$ scattering, the relative quark/gluon structure of the photon can be determined. Interactions between the almost-real photons produced by bremsstrahlung are determined primarily by interacting gluons in the ratio of approximately 70% gluons to 30% quarks. At higher $\sqrt{s}$, the gluon component should be more predominant. Thus, if real photons from laser backscattering are used, we expect to find an almost pure gluon-constituted photon (90%g/10%q) [24].

3.5 $\gamma^*\gamma^*$ scattering—QCD dynamics

Double-tagged virtual photon scattering completes the study of the photon at the linear collider by allowing the evolution of photon structure to be studied in an almost background-free environment. The Q^2 of each of the scattered leptons (denoted Q_1^2 and Q_2^2) is measured in the forward electromagnetic tagging calorimeters. By requir-

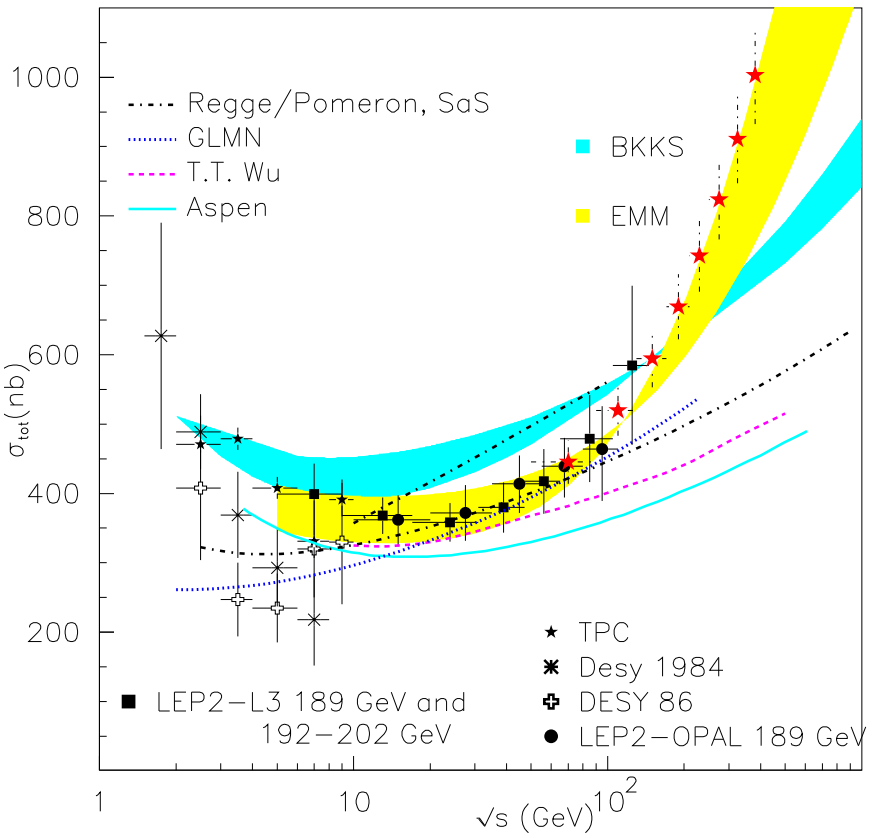

Figure 7.6: $\sigma_{\rm tot}$ versus $\sqrt{s}$ at a LC (large stars) compared to existing data and various models.

ing the ratio $Q_1^2/Q_2^2 \sim 1$, production of hadrons in the region between the two virtual photons through traditional DGLAP evolution is suppressed. This suppression grows stronger as the rapidity separation, Y, between the two virtual photons increases. At large values of Y, any signal above the small DGLAP background points to alternative forms of structure function evolution, *e.g.*, to the $\ln(1/x)$ evolution of BFKL [25]. Virtual photon scattering at a linear collider provides perhaps the cleanest environment in which to study BFKL physics [26,27].

With total center-of-mass energy $\sqrt{s}$ and photon virtuality Q^2, BFKL effects are expected in the kinematic region where the square of the photon-photon invariant mass (or, equivalently, the hadronic final-state system) is large, and

$$s \gg Q^2 \gg \Lambda_{QCD}^2.$$

At fixed order in QCD, the dominant process is four-quark production with t-channel gluon exchange. Each photon couples to a quark box, and the quark boxes are

connected via the gluon. The corresponding BFKL contribution arises from diagrams in which the t-channel gluon becomes a gluon ladder. At lepton-hadron or hadron-hadron colliders, the presence of hadrons in the initial state can complicate or even mask BFKL effects.

The largest values of Y are obtained at low $Q^2_{1,2}$, again emphasizing the need for the electromagnetic tagging calorimeters to be positioned as close to the beampipe as possible. Figure 7.7 shows the substantially greater reach in Y available to the 500 GeV LC relative to that of LEP2 running at 189 GeV.

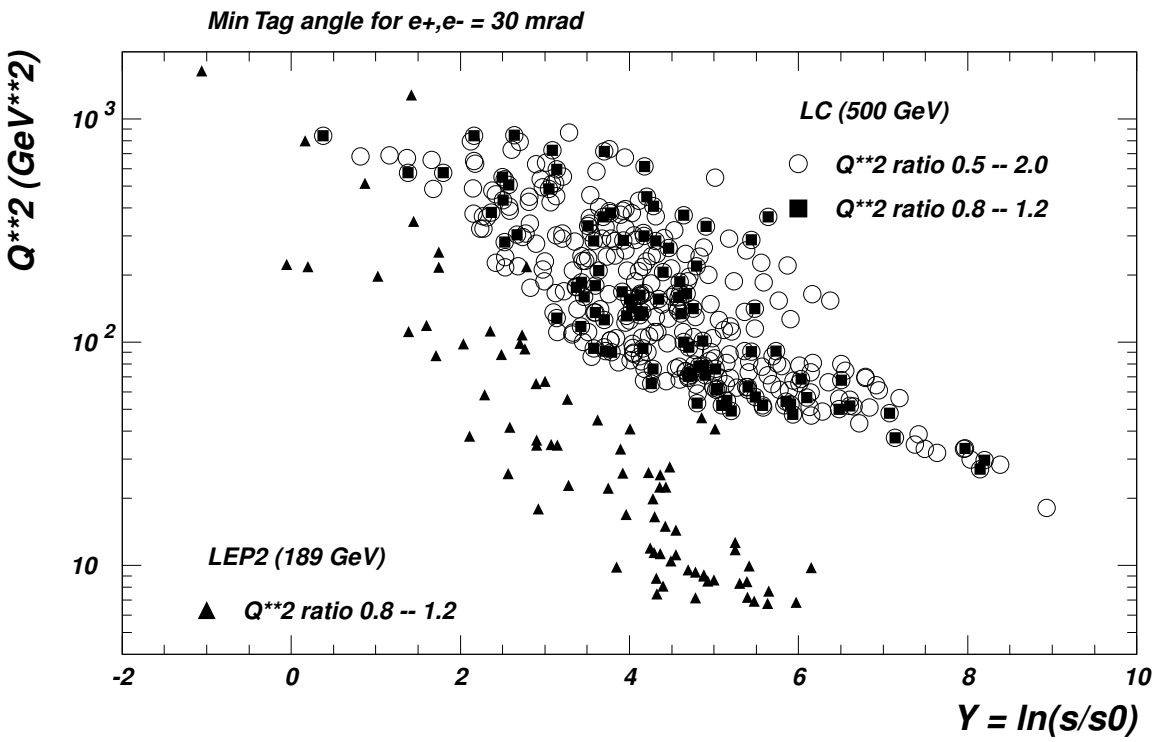

Figure 7.7: Q^2 versus Y for a 500 GeV LC compared to LEP2.

Experiments at LEP have looked for BFKL effects in virtual photon scattering [28]. The data tend to lie between the predictions of fixed-order QCD and analytic solutions to the BFKL equation (asymptotic full-order QCD). However, the data were compared to the asymptotic QCD prediction in a non-asymptotic regime [29], so the disagreement with QCD is not surprising. In contrast, a linear collider will be expected to reach closer to the asymptotic regime, providing a more definitive test of BFKL evolution. Improved predictions are also on the way with the development of BFKL Monte Carlo programs that incorporate kinematic constraints, such as [30]. On the more theoretical front, next-to-leading log corrections have been calculated

and found to be large, but the source of the large corrections is understood and they are being brought under control; see [31] for a review and references.

3.6 Summary of two-photon physics

The study of two-photon physics from e^+e^- collisions has grown tremendously in the past several years of higher-energy LEP2 running and will continue to provide a wealth of precision measurements at a future e^+e^- linear collider. Using combinations of tagged and untagged bremsstrahlung photons, aspects of real and virtual photon structure will be addressed, especially F_2^γ at high Q^2, the relative quark/gluon content of the photon from dijets, and possible BFKL effects in QCD evolution.

With laser-backscattered real photons, the highest energies available at the linear collider can be fully exploited. F_2^γ can be measured at very low x, which in combination with high Q^2 measurements from bremsstrahlung photons, will map out a kinematic region in photon structure as extensive as that known for the proton. The total $\gamma\gamma$ cross section will also be measured at the highest $\sqrt{s}$ available at the linear collider, leading to understanding of the dominant mechanisms responsible for this interaction.

Finally, with combinations of lepton and photon polarization, BFKL effects can be enhanced and the first measurements of polarized structure functions of the photon can be made.

4 Overall summary and conclusions

The high-energy linear collider offers a unique program of QCD and related two-photon studies. The strong coupling constant α_s can be measured at high Q^2 to a precision approaching $\pm 1\%$, free of the initial-state ambiguities that make the corresponding determination at a hadron collider substantially less precise, and allowing for substantial improvements in the determination of the running of the QCD coupling strength, as well as its extrapolation to the GUT scale. Constraints on the strong coupling properties of the top, providing sensitivity to a number of new physics scenarios inspired by the large mass of the top quark, can be made as much as an order of magnitude more stringent at an e^+e^- collider than at a proton collider of equivalent reach.

In two-photon reactions, the precisely defined state of the incoming electron and positron beams permits the kinematic properties of the interacting virtual and nearly on-shell photons to be inferred from the properties of the recoiling electrons. This in turn allows for a unique program of photon structure and strong-force dynamics which cannot be emulated by any other proposed facility. In addition, the possibility of precisely controlled real photon beams from the Compton backscattering of polarized laser light opens up further vistas in the exploration of photon structure, and may

allow the resolution of long-standing questions regarding the energy evolution of the photon-photon total cross section. Again, these studies are only possible within the larger context of an e^+e^- linear collider program.

Together, these physics topics present a unique and compelling program of strong-interaction studies at a high-energy linear collider, one that adds substantial weight to the promise of the proposed linear collider physics program.

References

[1] See, *e.g.*, S. Bethke, J. Phys. **G26**: R27 (2000).

[2] See, *e.g.*, P. N. Burrows, in Proc. XXVIII International Conference on High Energy Physics, Warsaw, Poland, July 25-31 1996, Eds. Z. Adjuk, A. K. Wroblewski, World Scientific 1997, p. 797.

[3] S. Bethke, in Proc. Workshop on Physics and Experiments with Linear e^+e^- Colliders, 26-30 April 1993, Waikoloa, Hawaii; World Scientific, Eds. F. A. Harris *et al.*

[4] B. Schumm, SCIPP-96-45, hep-ex/9612013 (1996).

[5] B. A. Schumm and A. S. Truitt, to appear in the proceedings of the 5th International Linear Collider Workshop (LCWS 2000), Fermilab, Batavia, Illinois, 24-28 Oct 2000; hep-ex/0102020.

[6] O. Biebel, PITHA 99/40, MPI-PhE/99-17, LC-PHSM-2000-003, hep-ex/9912051, Phys. Rept. **340**, 165 (2001).

[7] See, *e.g.*, OPAL Collaboration, OPAL Physics Note PN377.

[8] S. Catani *et al.*, Nucl. Phys. **B407**, 3 (1993).

[9] Z. Bern, L. Dixon, and D.A. Kosower, JHEP **0001**, 027 (2000).

[10] T. Gehrmann and E. Remiddi, Nucl. Phys. **B601**, 248, 287 (2001), hep-ph/0008287, hep-ph/0101124.

[11] See, *e.g.*, M. Neubert, Nucl. Phys. **B463**, 511 (1996); G. Altarelli, P. Nason, G. Ridolfi, Z. Phys. **C68**, 257 (1995).

[12] RG trajectories calculated in P. Langacker and N. Polonsky, Phys. Rev. **D52**, 3081 (1995).

[13] T. G. Rizzo, hep-ph/9605361.

[14] T. G. Rizzo, hep-ph/9506351.

[15] D. Atwood, A. Kagan, and T. G. Rizzo, Phys. Rev. **D52**, 6264 (1995).

[16] S. R. Magill, in Proc. Worldwide Study on Physics and Experiments with Future Linear e^+e^- Colliders, Sitges, Barcelona, Spain, April 28-May 5, 1066 (1999).

[17] R. Barate *et al.* (ALEPH), Phys. Lett. **B458**, 152 (1999); M. Acciarri *et al.* (L3), Phys. Lett. **B436**, 403 (1998); K. Ackerstaff *et al.* (OPAL), Phys. Lett. **B412**, 225 (1997); P. Abreu *et al.* (DELPHI), Zeit. Phys. **C69**, 223 (1996).

[18] V. G. Serbo, Proc. International Workshop on High Energy Photon Colliders, DESY Hamburg, Germany, June 14-17, 2000, to be published in Nucl. Inst. Meth. A., and references therein.

[19] T. Sjöstrand, Comp. Phys. Comm. **82**, 74 (1994).

[20] S. R. Magill, talk given at 2nd International Workshop on High Energy Photon Colliders, Fermilab, USA, March 14-17, 2001.

[21] J. Breitweg *et al.* (ZEUS), Eur. Phys. Jour. **C6**, 41 (1998); C. Adloff *et al.* (H1), Phys. Lett. **B462**, 440 (1999).

[22] J. Breitweg *et al.* (ZEUS), DESY 01-018 (February 2001), accepted by Phys. Lett. B; C. Adloff *et al.* (H1), DESY 00-181 (December 2000), submitted to Eur. Phys. J. C.

[23] R. M. Godbole and G. Pancheri, Proc. International Linear Collider Workshop (LCWS2000), Fermilab, USA, October 26-30, 2000.

[24] T. Wengler and A. De Roeck, Proc. International Workshop on High Energy Photon Colliders, DESY Hamburg, Germany, June 14-17, 2000, to be published in Nucl. Inst. Meth. A.

[25] L. N. Lipatov, Sov. J. Nucl. Phys. **23**, 338 (1976); E. A. Kuraev, L. N. Lipatov and V. S. Fadin, Sov. Phys. JETP **45**, 199 (1977); Ya. Balitsky and L. N. Lipatov, Sov. J. Nucl. Phys. **28**, 822 (1978).

[26] S. J. Brodsky, F. Hautmann and D. E. Soper, Phys. Rev. **D56**, 6957 (1997).

[27] M. Boonekamp, A. De Roeck, C. Royon and S. Wallon, Nucl. Phys. **B555**, 540 (1999) [hep-ph/9812523].

[28] See, *e.g.*, A. De Roeck, Nucl. Phys. Proc. Suppl. **99**, 144 (2001) and references therein.

[29] L. H. Orr and W. J. Stirling, Proc. 30th International Conference on High-Energy Physics (ICHEP 2000), Osaka, Japan, 27 Jul - 2 Aug 2000, hep-ph/0012198.

[30] C. R. Schmidt, Phys. Rev. Lett. **78** 4531 (1997); L. H. Orr and W. J. Stirling, Phys. Rev. **D56** 5875 (1997).

[31] G. P. Salam, Acta Phys. Polon. **B30**, 3679 (1999); Proc. 35th Rencontres de Moriond: QCD and High Energy Hadronic Interactions, Les Arcs, Savoie, France, 18-25 March 2000, hep-ph/0005304, and references therein.